

# Journal of Materials Chemistry C

Accepted Manuscript



This is an *Accepted Manuscript*, which has been through the Royal Society of Chemistry peer review process and has been accepted for publication.

*Accepted Manuscripts* are published online shortly after acceptance, before technical editing, formatting and proof reading. Using this free service, authors can make their results available to the community, in citable form, before we publish the edited article. We will replace this *Accepted Manuscript* with the edited and formatted *Advance Article* as soon as it is available.

You can find more information about *Accepted Manuscripts* in the [Information for Authors](#).

Please note that technical editing may introduce minor changes to the text and/or graphics, which may alter content. The journal's standard [Terms & Conditions](#) and the [Ethical guidelines](#) still apply. In no event shall the Royal Society of Chemistry be held responsible for any errors or omissions in this *Accepted Manuscript* or any consequences arising from the use of any information it contains.

## ARTICLE

# A new red phosphor BaGeF<sub>6</sub>:Mn<sup>4+</sup>: hydrothermal synthesis, photo-luminescent properties, and its application in warm white LED devices

Cite this: DOI: 10.1039/x0xx00000x

Received 00th December 2014,  
Accepted 00th January 2015

DOI: 10.1039/x0xx00000x

www.rsc.org/

Qiang Zhou,<sup>a</sup> Yayun Zhou,<sup>a</sup> Yong Liu,<sup>a</sup> Lijun Luo,<sup>a</sup> Zhengliang Wang,<sup>\*a</sup> Jinhui Peng,<sup>a</sup> Jing Yan,<sup>b</sup> and Mingmei Wu<sup>\*b</sup>

In this work, we report a new and efficient red phosphor BaGeF<sub>6</sub>:Mn<sup>4+</sup> (denoted as BGFM) by hydrothermally etching BaCO<sub>3</sub> and GeO<sub>2</sub> in HF solution with an optimized KMnO<sub>4</sub> concentration. The crystal structure and morphology were characterized by powder X-ray diffraction (XRD), scanning electron microscopy (SEM) and energy-dispersive X-ray spectroscopy (EDS) in details. The influence of synthesis conditions on its photo-luminescent (PL) properties has been investigated comprehensively. It can present a broad adsorption and sharp emissions in blue and red ranges respectively. The white LED device made of blue GaN chip merged with YAG:Ce-BGFM mixture presents warmer white light than that merged with only one YAG:Ce component.

## Introduction

Over the past decade, the white light-emitting diodes (WLEDs) have been a topic of interest to scientists and engineers due to their high energy efficiency, long lifetime, and environmental friendly properties.<sup>1-3</sup> Generally, the most popular WLED is fabricated from blue GaN chip and yellow-emitting Y<sub>3</sub>Al<sub>5</sub>O<sub>12</sub>:Ce<sup>3+</sup> (YAG:Ce) phosphor, which can absorb blue light excited from the GaN chip to emit high luminous efficiency white light.<sup>4,5</sup> However, the white light possessed by this kind of WLED lacks red emission component,<sup>6,7</sup> which results in it hard for indoor lighting application because of high correlated colour temperature (CCT > 6,000 K) and low colour rendering index (CRI, R<sub>a</sub> < 80).<sup>8-11</sup> To solve this problem, enormous research efforts have been devoted to develop red phosphors, such as Mn<sup>4+</sup> activated ones with intense broad excitation band in blue region and sharp emission in red region. The optical performance of WLEDs can be improved by mixing them with YAG:Ce phosphor.<sup>12-14</sup>

Mn<sup>4+</sup> doped materials, especially aforementioned Mn<sup>4+</sup> activated red phosphors have been widely investigated since its distinct <sup>2</sup>E → <sup>4</sup>A<sub>2</sub> transition in symmetrically octahedral crystal field, resulting in the phosphor broad adsorption bands at 380-490 nm and sharp emission peaks at 610-760 nm.<sup>15,16</sup> A typical example is Mn<sup>4+</sup> activated Mg<sub>2</sub>TiO<sub>4</sub> red phosphor.<sup>17,18</sup> However, its emission located between 650 and 720nm, which are too far red-shifted for efficient warm WLEDs with a high luminous efficiency. To overcome this drawback, very recently, a series of fluoride A<sub>2</sub>XF<sub>6</sub>:Mn<sup>4+</sup> red phosphors (A = K, Na, Ba and B =

Si, Ti), based on a facile one-step synthesis have been reported.<sup>19-24</sup> For example, Liu demonstrated a one-step co-precipitation approach to synthesize Na<sub>2</sub>SiF<sub>6</sub>:Mn<sup>4+</sup> and K<sub>2</sub>SiF<sub>6</sub>:Mn<sup>4+</sup> red phosphors from a silicon fluoride solution using H<sub>2</sub>O<sub>2</sub> to reduce Mn<sup>7+</sup> to Mn<sup>4+</sup> at room temperature.<sup>19</sup> Qiu reported a facile redox reaction to fabricate K<sub>2</sub>SiF<sub>6</sub>:Mn<sup>4+</sup> red phosphor in HF/KMnO<sub>4</sub> solution at room temperature.<sup>21</sup> A series of single phase A<sub>2</sub>XF<sub>6</sub>:Mn<sup>4+</sup> red phosphors, such as K<sub>2</sub>SiF<sub>6</sub>:Mn<sup>4+</sup>, BaTiF<sub>6</sub>:Mn<sup>4+</sup> and BaSiF<sub>6</sub>:Mn<sup>4+</sup> have been prepared by a one-pot synthesis including hydrothermal and/or chemical etching route.<sup>22-24</sup> Despite these successes, to the best of our knowledge, the feasible approach for the direct preparation of BaGeF<sub>6</sub>:Mn<sup>4+</sup> (BGFM) red phosphor, has not yet been reported.

In this paper, for the first time, we present an efficient one-step hydrothermal approach to fabricate single-phase BGFM red phosphor with micro-rod morphology. The influence of the reaction parameters, such as the concentration of starting materials, the reaction temperature and time, on the PL properties of the BGFM red phosphor has been investigated systematically. The optimal reaction condition is achieved and the optimized BGFM red phosphor emits intensive red light under blue light excitation. The as-fabricated WLED with YAG:Ce-BGFM mixture exhibits warmer white light than that with only one YAG:Ce component.

## Experimental

### Materials and synthesis

All source materials in this work, including hydrofluoric acid, barium carbonate, germanium oxide, potassium permanganate, yttrium oxide, cerium oxide and aluminium hydroxide were of analytical grade and without any further purification prior to use. Red phosphors BGFM were synthesized *via* a one-pot hydrothermal treatment from BaCO<sub>3</sub>, GeO<sub>2</sub> and KMnO<sub>4</sub> in HF solution. In a typical synthesis, 0.494 g of BaCO<sub>3</sub>, 0.262 g of GeO<sub>2</sub> and 0.079 g of KMnO<sub>4</sub> were weighted and added into a Teflon cup containing 50.0 ml of HF solution with magnetic stirring for 30 min. The hydrothermal synthesis was conducted at 180 °C for 8.0 hours. After the autoclave was cooled down naturally to room temperature, the resulting solid product was collected carefully from the cup, washed extensively with distilled water and methanol for several times, and dried at 60 °C for 12.0 hours.

Yellow phosphor YAG:Ce was synthesized according to the procedures described in literature with minor modifications.<sup>25</sup> The stoichiometric mixtures of Y<sub>2</sub>O<sub>3</sub>, Al(OH)<sub>3</sub> and CeO<sub>2</sub> were ground and fired at 1300 °C for 8.0 h in reducing atmosphere (N<sub>2</sub>: H<sub>2</sub> = 95 : 5).

The LEDs were fabricated by coating the phosphors and epoxy resin mixture (mass ratio is 1:1) on GaN chips (~ 460 nm).

### Characterizations

Initially, Powder X-ray diffraction (XRD) was used to investigate the crystal structure of the as-prepared product with an X-ray diffractometer using Cu K<sub>α</sub> radiation ( $\lambda = 0.15406$  nm) and a graphite monochromator from 15° to 70°. The surface morphologies and structures of the obtained phosphors were observed by a scanning electron microscopy (SEM, FEI Quanta 400 Thermal FE Environment scanning electron microscopy) with an attached energy-dispersive X-ray spectrometer (EDS). The valence state was examined by a Scanning X-ray photoelectron spectroscopy Microprobe system (XPS, Phi5000 Versaprobe-II, Ulvac-Phi) with an Al target working at 15 kV. The Diffuse Reflectance Ultraviolet-Visible spectrum (DRS) was collected on an Cary 5000 UV-Vis-NIR spectrophotometer, and the luminescence decay curve was obtained from an FLS920 fluorescence spectrophotometer. PL properties were examined on a Cary Eclipse FL1011M003 (Varian) spectrofluorometer with the xenon lamp as excitation source. The performance of WLEDs was recorded on a high accurate array spectrometer (HSP6000).

## Results and discussion

### Phase, composition and morphology

The XRD patterns of the hydrothermally synthesized BaGeF<sub>6</sub> with and without Mn<sup>4+</sup> doping are shown in Fig. 1, along with its corresponding standard diffraction card. It is obvious that in Fig. 1a, all the diffraction peaks that appear for the as-prepared

products agree well with the standard BaGeF<sub>6</sub> card (JCPDS No. 74-0924, space group *R*-3m,  $a = b = c = 4.83$  nm), which indicates each product is a single pure phase of BaGeF<sub>6</sub>. Fig. 1b displays the BGFM product hydrothermally treated with 10.0 mmol·L<sup>-1</sup> KMnO<sub>4</sub> and 40 % (v/v) HF solution at 180 °C for 8.0 h. As similar as curve a, it is also of single pure phase, which means the doping of Mn<sup>4+</sup> does not change the crystal structure of this BaGeF<sub>6</sub> host. That is because Mn<sup>4+</sup> not only has the same valence state as Ge<sup>4+</sup>, but also the identical ionic radius with Ge<sup>4+</sup> (0.53 Å, CN = 6 vs. 0.53 Å, CN = 6). This results in charge balance between Ge<sup>4+</sup> and Mn<sup>4+</sup> in BGFM and similar profile between Fig. 1b and Fig. 1a.

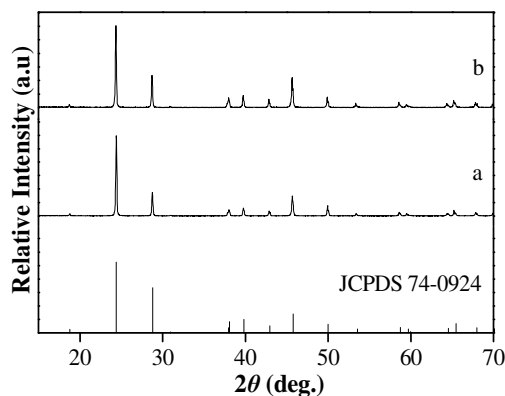


**Fig. 1** Representative XRD patterns of the (a) BaGeF<sub>6</sub> host and BGFM product prepared at 180 °C for 8.0 h with 10.0 mmol·L<sup>-1</sup> KMnO<sub>4</sub> and 40 % (v/v) HF solution.

To determine whether Mn<sup>4+</sup> ions were doped into the BaGeF<sub>6</sub> matrix, the luminescent properties of the above obtained BGFM product were examined and shown in Fig. 2a. It demonstrated two broadband excitation peaks, according to the Tanabe-Sugano diagram, which are attributable to the spin-allowed and parity-forbidden transitions from ground state <sup>4</sup>A<sub>2g</sub> to excited state <sup>4</sup>T<sub>1g</sub> and <sup>4</sup>T<sub>2g</sub> of Mn<sup>4+</sup> in the UV and blue region respectively.<sup>21</sup> The corresponding emission spectrum exhibited three strong peaks locating in the red region, which was a typical property of Mn<sup>4+</sup> ion-activated phosphors as reported previously.<sup>26,27</sup> This strongly indicates that the Mn<sup>4+</sup> ions have been doped into the BaGeF<sub>6</sub> matrix.

Fig. 2b-c exhibits the representative SEM and energy-dispersive X-ray spectroscopy (EDS) results of the particulate BGFM red phosphor prepared from hydrothermal treatment of BaCO<sub>3</sub>, GeO<sub>2</sub> and KMnO<sub>4</sub> in 40 % (v/v) HF solution. The SEM picture illustrates that a number of rod-shaped crystals with smooth surfaces are present in the as-synthesized BGFM product. Closely observing the tips of these rods, each rod has a diameter about 0.2 μm and length around 2 μm. Actually, the morphologies of all obtained BGFM products prepared from different concentration of HF are similar to Fig. 2b (see Fig. S1 in ESI<sup>†</sup>). The EDS spectra of Fig. 2c clearly recognized the peaks of F, Ge, Ba, and Mn elements, which also can be identified from the XPS profile (Fig. S2 in ESI<sup>†</sup>), suggesting that Mn element has been indeed doped into the matrix lattice to occupy the Ge lattice site. This result further verifies that the

$Mn^{4+}$  ions are active centres in  $BaGeF_6$  to emit red light under blue light excitation. Actually, the molar concentration of Mn in this product, which also indicated by the XPS result, is very low. Moreover, the absence of oxygen peak in the EDS result implies that there are no presence of  $MnO_2$  in the hydrothermal reaction, which was identical with the previous work<sup>20</sup>.

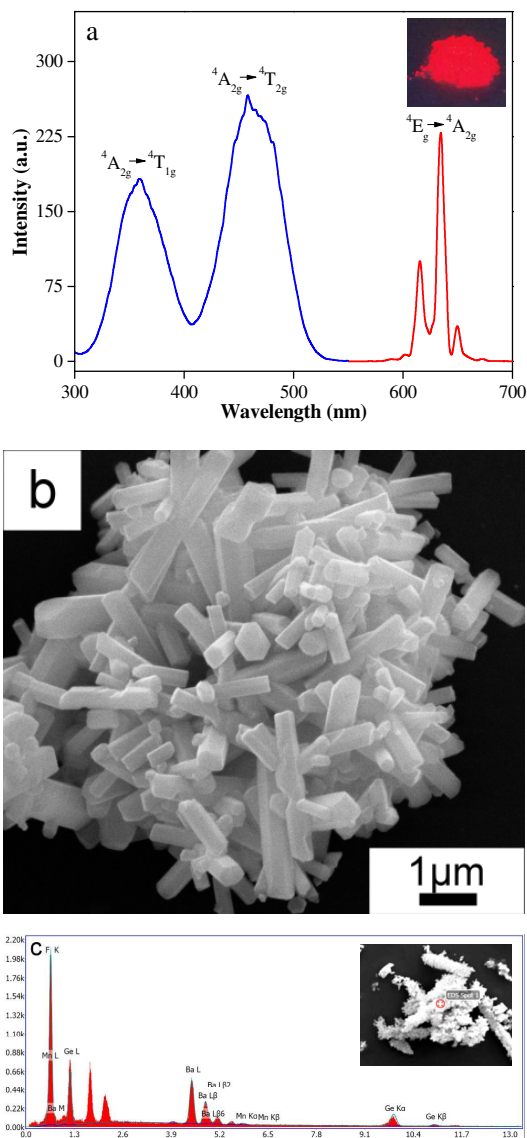


**Fig. 2** (a) The excitation and emission spectra with a typical photo image excited under a UV lamp, (b) SEM picture, (c) EDS data of the as-synthesized BGFM red phosphor obtained from  $10.0 \text{ mmol}\cdot\text{L}^{-1}$   $KMnO_4$  and 40 % (v/v) HF solution at  $180^\circ\text{C}$  for 8.0 h.

### Optical properties and application in WLEDs

Because of the same ionic radius and charge balance,  $Mn^{4+}$  ions can substitute octahedral  $Ge^{4+}$  ionic sites in  $BaGeF_6$  to form the BGFM red phosphor, resulting in its strong absorption in blue region. This was also observed in the diffuse reflection spectra (DRS) (Fig. S3 in ESI<sup>†</sup>), which revealed a strong adsorption peak at 457 nm. This phenomenon is a strong indication for its potential application in blue GaN chips.

For a crystal synthesized from hydrothermal route, it is necessary to investigate the influence of some general reaction parameters, such as the concentration of starting materials, the reaction temperature and time, on its PL properties. Therefore, different concentration of HF, from 10 % to 40 % (v/v) was employed to investigate the PL properties of BGFM red phosphors. Fig. 3 exhibits the excitation and emission spectra prepared with different HF concentrations. It is clear that the shapes of these excitation spectra are similar, each of which is composed of two broadband peaks. As illustrated above, the broad excitation bands are attributed to the spin-allowed and parity-forbidden transitions  $^4A_2-^4T_{1g,2g}$  of  $Mn^{4+}$  respectively. The stronger excitation locates at 460 nm, which matches perfectly with the blue emission of GaN chip ( $\sim 460 \text{ nm}$ ).

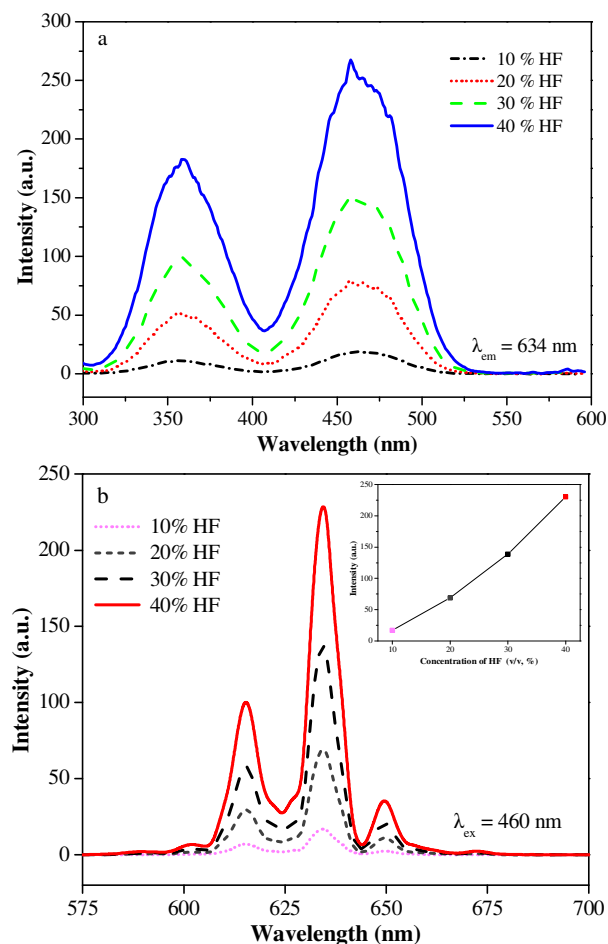


**Fig. 3** (a) Excitation and (b) emission spectra of red phosphor BGFM obtained at  $180^\circ\text{C}$  for 8.0 h with  $10.0 \text{ mmol}\cdot\text{L}^{-1}$   $KMnO_4$  and (a) 10 %, (b) 20 %, (c) 30 % and (d) 40 % (v/v) HF, the insert is the relationship between HF concentration and the relative emission intensity of BGFM.

Fig. 3b shows a series of corresponding emission spectra of the BGFM phosphors under 460 nm light excitation. Three emission peaks locating at 615, 634 and 649 nm strongly indicates the emitted light is red, which are identified as the anti-strokes and strokes transitions between  $^2E$  and  $^4A_2$  levels of  $Mn^{4+}$  respectively.<sup>22-24</sup> Among all the emission peaks, the strongest peak locates at 634 nm. Moreover, Fig. 3b exhibits

the effect of HF concentration on the emission intensity of BGFM. It is obvious that the emission intensity increases with the HF concentration, until it reaches 40 % (v/v), at which the obtained BGFM phosphor emits stronger red light than that of other samples. That may be because higher HF concentration is beneficial for the formation of stable  $\text{MnF}_6^{2-}$  group. With the highest HF concentration, the obtained BGFM phosphor emits the most brightness red light. Therefore, the following experiments were conducted in this 40 % (v/v) HF environment. The relationship between HF concentration and the relative emission intensity of BGFM phosphor is illustrated in the insert of Fig. 3b.

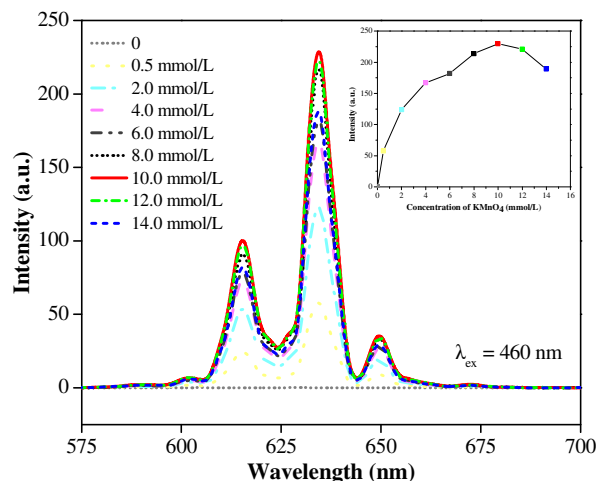


**Fig. 4** Emission spectra of BGFM red phosphors obtained from 40 % (v/v) HF with different concentration of  $\text{KMnO}_4$  at 180 °C for 8.0 h, the insert is the relationship between the concentration of  $\text{KMnO}_4$  and the relative emission intensity of BGFM.

As we know, the doping amount of a phosphor plays a very important role in its PL properties. But in this work, it is hard to accurately decide the doping amount of  $\text{Mn}^{4+}$  in BGFM products. Thus from a practical point of view, it is very important to investigate the effect of  $\text{KMnO}_4$  concentration on the PL properties of the as-synthesized BGFM red phosphors. It can be clearly observed that the emission spectra in Fig. 4 also share the similar shape. Without the addition of  $\text{KMnO}_4$ , no emission peaks can be observed. Adding a small amount of  $\text{KMnO}_4$  into the reaction system, the emission intensity sharply increased. With the addition of  $\text{KMnO}_4$ , the emission peaks gradually increased until it reaches 10.0  $\text{mmol}\cdot\text{L}^{-1}$ , at which the BGFM emits the strongest red light and the CIE (Commission Internationale de l'Éclairage, International Commission on Illumination) chromaticity coordinates are  $x = 0.695$ ,  $y = 0.305$ . This value is close to the “ideal red” of NTSC (National Television Standard Committee,  $x = 0.67$ ,  $y = 0.33$ , Fig. S4 in ESI†). Furthermore, the strongest peak locating at 634 nm is very close to the ideal red (620 nm) in terms of luminous efficacy of white emitting LEDs. With a continual increase of  $\text{KMnO}_4$  concentration, the emission contrarily dropped, which may be due to the concentration quenching of  $\text{Mn}^{4+}$  in  $\text{BaGeF}_6$  crystal lattice.<sup>28</sup> Relationship between the  $\text{KMnO}_4$

concentration and the relative emission intensity of BGFM phosphor is inserted in Fig. 4.

Fig. 5 investigates the effect of synthesis temperature on the PL property of the obtained BGFM phosphor. Similar as illustrated above, all of the BGFM phosphors emit red light as well, and the emission intensity can be enhanced by increasing the reaction temperature from 100 °C to 180 °C, which is probably due to the improved crystallization at higher temperature.<sup>23</sup> However, with the further increase of reaction temperature, the emission intensities decreases as shown in Fig. 5. It is possible some structures tend to deteriorate at much higher temperature. The reaction time influenced little on the PL properties of the BGFM phosphors (Fig. S5 in ESI†) and the best reaction period is 8.0 h. Therefore, according to the results obtained above, the optimized reaction condition is: 10.0  $\text{mmol}\cdot\text{L}^{-1}$   $\text{KMnO}_4$ , 40 % (v/v) HF, reacted at 180 °C for 8.0 h. The thermal behavior and decay curve of the optimized BGFM red phosphor is shown in Fig. S6 and S7 (ESI†). The decomposition temperature of BGFM is about 519.6 °C and its decay curve is well fitted into single-exponential function with a lifetime  $\tau$  value of 5.89 ms.

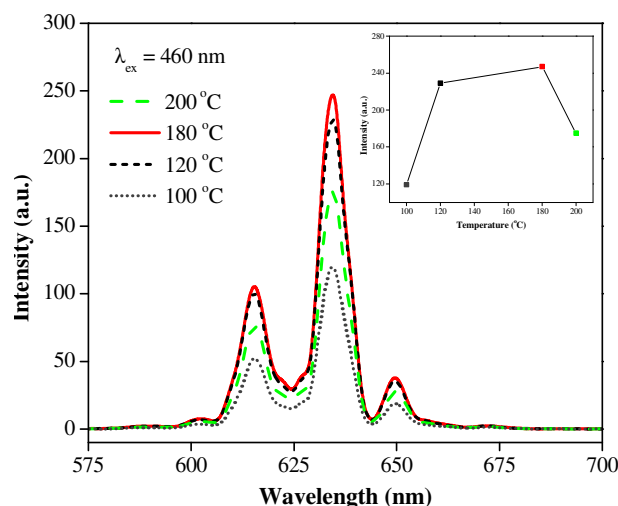


**Fig. 5** Emission spectra of BGFM red phosphors obtained from 40 % (v/v) HF and 10.0  $\text{mmol}\cdot\text{L}^{-1}$   $\text{KMnO}_4$  at (a) 100 °C, (b) 120 °C, (c) 180 °C and (d) 200 °C for 8.0 h, the insert is the relationship between reaction temperature and the relative emission intensity of BGFM.

Fig. 6 shows the electro-luminescent spectra of the GaN chip, the LED based on BGFM, YAG:Ce, YAG:Ce-BGFM mixture under 20 mA current excitation. The peak at  $\sim 460$  nm can be attributable to the emission of GaN chip (Fig. 6a) while the peaks at 634 nm are due to the emission of BGFM phosphor (Fig. 6b), which can make the bright red light be clearly observed by naked eyes (insert of Fig. 6b). The difference between two WLEDs was shown in Fig. 6c-d. Obviously, the red emission in Fig. 6d is very clear, which means the addition of BGFM is favourable for improving the CRI and CCT levels of the YAG:Ce type WLED. The performance is summarized in Tab. S1 (ESI†). Briefly, the white light emitted from the GaN-YAG:Ce-BGFM type WLED is warmer than that from the

GaN-YAG:Ce system (CCT ~ 4210K, CRI ~ 84, LE ~ 52.21 lm/W vs. CCT ~ 6283K, CRI ~ 76, LE ~ 45.21 lm/W). It is worth pointing out that the luminous efficiency has also been enhanced with the use of BGFMs.

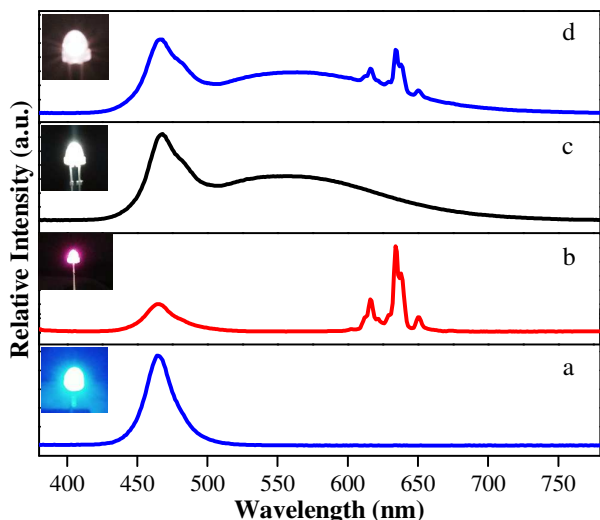


**Fig. 6** Electro-luminescent spectra of (a) the GaN chip, the LED based on (b) BGFMs, (c) YAG:Ce and (d) YAG:Ce-BGFMs mixture under 20 mA current excitation, the inserts are the corresponding light images.

## Conclusions

In summary, a class of  $\text{BaGeF}_6:\text{Mn}^{4+}$  red phosphors with micro-rod morphology have been prepared from  $\text{BaCO}_3$ ,  $\text{GeO}_2$  and  $\text{KMnO}_4$  in HF solution using a one-pot hydrothermal route. The influence of synthesis conditions, including the concentrations of  $\text{KMnO}_4$  and HF, synthesis temperature and time, on the photo-luminescent properties of the  $\text{BaGeF}_6:\text{Mn}^{4+}$  product, have been investigated in details. The optimal  $\text{BaGeF}_6:\text{Mn}^{4+}$  red phosphor can absorb broadband blue light and emit red light efficiently, which resulting in that the YAG:Ce-BGFMs based WLEDs display warmer white light than that of the YAG:Ce type. Therefore, the improved optical performance of WLEDs may find potential application in indoor lighting.

## Acknowledgements

We acknowledge the financial support of the National Natural Science Foundation of China (NSFC 21261027), the Natural Science Foundation of Yunnan Province, and Department of Yunnan Education (Grants 2014FB147 and 2014Y253), the Joint Funds of the National Natural Science Foundation of China and Guangdong Province (U1301242), Research Fund for the Doctoral Program of Higher Education of China (20130171130001), and Guangdong Province for industrial applications of rare earth materials (2012B09000026).

## Notes and references

<sup>a</sup> Key Laboratory of Comprehensive Utilization of Mineral Resources in Ethnic Regions, Key Laboratory of Resource Clean Conversion in Ethnic Regions, Education Department of Yunnan, School of Chemistry

and Biotechnology, Yunnan Minzu University, Kunming, 650500, P. R. China, E-mail: wangzhengliang@foxmail.com

<sup>b</sup> MOE Key Laboratory of Bioinorganic and Synthetic Chemistry, School of Chemistry and Chemical Engineering, Sun Yat-Sen (Zhongshan) University, Guangzhou, 510275, P. R. China, E-mail: ceswmm@mail.sysu.edu.cn

- 1 E. F. Schubert and J. K. Kim, *Science*, 2005, **308**, 1274.
- 2 H. Daicho, T. Iwasaki, K. Enomoto, Y. Sasaki, Y. Maeno, Y. Shinomiya, S. Aoyagi, E. Nishibori, M. Sakata, H. Sawa, S. Matsuishi and H. Hosono, *Nat. Commun.*, 2012, **3**, 1132.
- 3 W. T. Chen, H. S. Shen, R. S. Liu and J. P. Attfield, *J. Am. Chem. Soc.*, 2012, **134**, 8022.
- 4 X. Yan, W. Li, X. Wang and K. Sun, *J. Electrochem. Soc.*, 2012, **159**, 195.
- 5 D. W. Wen, J. J. Feng, J. H. Li, J. X. Shi, M. M. Wu and Q. Su, *J. Mater. Chem. C*, 2015, DOI: 10.1039/C4TC02406K.
- 6 Q. H. Zeng, P. He, M. Pang, H. B. Liang, M. L. Gong and Q. Su, *Solid State Commun.*, 2009, **149**, 880.
- 7 P. H. Chuang, C. C. Lin, H. Yang and R. S. Liu, *J. Chin. Chem. Soc.*, 2013, **60**, 801.
- 8 T. S. Chan, R. S. Liu and I. Baginskiy, *Chem. Mater.*, 2008, **20**, 1215.
- 9 K. A. Denault, N. C. George, S. R. Paden, S. Brinkley, A. A. Mikhailovsky, J. Neufeind, S. P. DenBaars and R. Seshadri, *J. Mater. Chem.*, 2012, **22**, 18204.
- 10 G. G. Li, D. L. Geng, M. M. Shang, C. Peng, Z. Y. Cheng and J. Lin, *J. Mater. Chem.*, 2011, **21**, 13334.
- 11 A. A. Setlur, W. J. Heward, Y. Gao, A. M. Srivastava, R. G. Chandran and M. V. Shankar, *Chem. Mater.*, 2006, **18**, 3314.
- 12 M. J. Lee, Y. H. Song, Y. L. Song, G. S. Han, H. S. Jung and D. H. Yoon, *Mater. Lett.*, 2015, **141**, 27.
- 13 H. M. Zhu, C. C. Lin, W. Q. Luo, S. T. Shu, Z. G. Liu, Y. S. Liu, J. T. Kong, E. Ma, Y. G. Cao, R. S. Liu and X. Y. Chen, *Nat. Commun.*, 2014, **5**, 4312 1.
- 14 J. H. Oh, H. Kang, Y. J. Eo, H. K. Park and Y. R. Do, *J. Mater. Chem. C*, 2015, **3**, 607.
- 15 Y. K. Xu and S. Adachi, *J. Appl. Phys.*, 2009, **105**, 013525.
- 16 R. Hoshino and S. Adachi, *J. Appl. Phys.*, 2013, **114**, 213502.
- 17 M. M. Medic, M. G. Brik, G. Drazic, Z. M. Antic, V. M. Lojpur, and M. D. Dramicanin, *J. Phys. Chem. C*, 2015, **119**, 724..
- 18 T. N. Ye, S. Li, X. Y. Wu, M. Xu, X. Wei, K. X. Wang, H. L. Bao, J. Q. Wang and J. S. Chen, *J. Mater. Chem. C*, 2013, **1**, 4327.
- 19 T. D. Nguyen, C. T. Dinh and T. O. Do, *ACS Nano*, 2010, **4**, 2263.
- 20 H. D. Nguyen, C. C. Lin, M. H. Fang and R. S. Liu, *J. Mater. Chem. C*, 2014, **2**, 10268.
- 21 C. X. Liao, R. P. Cao, Z. J. Ma, Y. Li, G. P. Dong, K. N. Sharafudeen and J. R. Qiu, *J. Am. Ceram. Soc.*, 2013, **96**, 3552.
- 22 L. F. Lv, X. Y. Jiang, S. M. Huang, X. A. Chen and Y. X. Pan, *J. Mater. Chem. C*, 2014, **2**, 3879.
- 23 X. Y. Jiang, Z. Chen, S. M. Huang, J. G. Wang and Y. X. Pan, *Dalton Trans.*, 2014, **43**, 9414.
- 24 L. L. Wei, C. C. Lin, M. H. Fang, M. G. Brik, S. F. Hu, H. Jiao and R. S. Liu, *J. Mater. Chem. C*, DOI: 10.1039/C4TC02551B.
- 25 A. Ikesue, T. Kinoshita, K. Kammata and K. Yoshida, *J. Am. Ceram. Soc.*, 1995, **78**, 225-228.
- 26 X. Y. Jiang, Y. X. Pan, S. M. Huang, X. A. Chen, J. G. Wang and G. K. Liu, *J. Mater. Chem. C*, 2014, **2**, 2301.

## ARTICLE

Journal Name

- 27 D. Sekiguchi, J. Nara and S. Adachi, *J. Appl. Phys.*, 2013, **113**, 183516.
- 28 Z. L. Wang, P. Cheng, Y. Liu, Y. Y. Zhou, Q. Zhou and J. M. Guo, *Opt. Mater.*, 2014, **37**, 277.

### Graphical Abstract

A new red phosphor  $\text{BaGeF}_6:\text{Mn}^{4+}$  prepared by a hydrothermal route shows intense red emission under blue light excitation, which may find application in warm white LED devices.

